

Calibration of Cascading Failure Simulation Models for Power System Risk Assessment

Blazhe Gjorgiev, Bing Li, Giovanni Sansavini

*Reliability and Risk Engineering Laboratory, Swiss Federal Institute of Technology, (ETH) Zürich
Zürich, Switzerland. E-mail: {gblazhe, libing, sansavig}@ethz.ch*

Recently a number of attempts have been made to validate and calibrate power system cascading failure simulation models. The objective of this paper is to assess the potential for model calibration. For that purpose, we propose a generic framework for the calibration of cascading failure analysis models. The framework is based on tuning the optimal values of model parameters, i.e. line/transformer tripping power-flow thresholds, which are usually diverse depending on the particular settings chosen by maintenance personnel. The framework application is exemplified by calibrating the parameters of a cascading failure model based on DC power flow (PF). The parameters are optimized through minimizing the difference between the probability distributions of historical blackout data and of the simulation results for the same electric power transmission system. The problem is casted as single-objective optimization and is solved using different optimization techniques. The efficiency of the proposed framework and the selected optimization techniques is demonstrated on the Western Electricity Coordinating Council (WECC) power transmission system. The obtained results show that by tuning model parameters optimally, one can achieve a good agreement between the simulation results and the historical data. These findings support the applicability of the cascading failure simulations to power system risk assessment.

Keywords: Power system, cascading failures, simulations, optimization, calibration, validation, risk.

1. Introduction

Recent wide-area blackouts such as the 2011 Southwest blackout in Arizona and South California (Ferc, 2012) and the record-breaking blackout in India (Romero, 2012), suggest that the concerns regarding the blackout threats in the transmission system are well grounded. In response to that, a growing number of analytical and simulation methods are emerging for studying the cascading failure in order to prevent and mitigate blackouts and improve the reliability of power grids (Li *et al.*, 2007). However, only a limited number of models undergo validation.

The benchmarking and validation of cascading failure analysis tools is challenging due to: 1) lack of knowledge of the system state and the contingencies when the cascading events happened; 2) difficulty to choose modeling assumptions; in the real cascading events, diverse set of cascade mechanisms can occur; 3) insufficient historical data used to calibrate the model parameters; indeed, comparing a model's results to historical data from real power systems is a useful validation method; 4) incomplete power system data; the validation of a particular model requires the use of a particular set of case data.

This paper aims to propose a methodology, which calibrates the parameters of a cascading failure analysis model (Li *et al.*, 2018a) against the

historical cascading outage data of a real electric power transmission system. The calibrated model is able to capture the important statistical characteristics of the historical blackout events and can be used to forecast possible future cascading events and to quantify the associated risks. Due to the many complicated mechanisms involved in cascading failure analysis, it is infeasible to adjust the simulation results by calibrating the model parameters through analytical approaches, and in most of previous validation works the parameters are chosen intuitively (Carreras *et al.*, 2013). In this paper, three optimization techniques, suitable for simulation-based optimization, are used, i.e. genetic algorithm (GA) (Goldberg, 1989), partial swarm pattern optimization (PSO-P) (Vaz and Vicente, 2007) and mesh adaptive direct search (MADS) (Audet and Dennis, 2006), for calibrating the parameters of the DC PF based cascading failure analysis. The benchmarking and validation of the cascading failure analysis is conducted by comparing the simulation results with the statistics of the historical cascades, i.e. the probability distribution of the blackout size, i.e. the fraction of the instantaneous power demand not served to the customers as a result of the blackout induced by the cascading outage.

The remainder of the paper is structured as follows: in Section 2 a DC PF based cascading

Proceedings of the 29th European Safety and Reliability Conference.

Edited by Michael Beer and Enrico Zio

Copyright © 2019 European Safety and Reliability Association.

Published by Research Publishing, Singapore.

ISBN: 978-981-11-2724-3; doi:10.3850/978-981-11-2724-3-0919-cd

failure analysis model is presented; in Section 3 the approach for calibrating and validating the cascading failure analysis model is elaborated; the results and analyses are shown in Section 4; the conclusions are given in Section 5.

2. DC PF Cascading Failure Analysis

In this Section, the DC PF cascading failure analysis is presented. It simulates the evolution of cascading events due to initial contingencies and quantifies the potential negative consequences of the cascade process.

Due to the large number of possible contingencies, the system operator should be able to quickly estimate the potential occurrence and impact of a cascading event in the transmission network. Model details must be traded off with the simulation time and accuracy. The model considers the most common propagation mechanism (Vaiman *et al.*, 2012), i.e., cascade of overloaded lines, and takes into account the frequency problem which are typically to occur in the cascading failure. The analysis neglects the transient behavior, which would require a real-time assessment e.g. rotor angle stability. Furthermore, it neglects the voltage instabilities in the system. It aims at estimating the power not supplied due to the cascading events, while using automatic frequency control and under frequency load shedding as defense mechanisms against cascade progression in the system. The model:

- 1) simulates critical scenarios which may trigger the cascading event. The random failure probability p for components of transmission lines and generators can be calibrated to generate reasonable probability distribution for combinations of component failure;
- 2) computes the load flow change on the transmission lines using a DC power flow algorithm;
- 3) employs frequency control of generators to restore the power generation/consumption balance in case of island operation, the frequency deviation are computed and the frequency control is modeled according to (Kundur *et al.*, 1994; Bing *et al.*, 2016);
- 4) performs automatic disconnection when the line reaches its rating (Staszewski and Rebizant, 2010; Sansavini *et al.*, 2014); normally, the transmission lines can keep working under overload conditions for hours, i.e. beyond their nameplate rating. In order to capture the diversity between nameplate rating and actual line operations, we can tune the

threshold for which the lines reach their failure limit in terms of a line tripping threshold α , which we calibrate as a model parameter;

- 5) conducts stability checks in island operation when the power imbalance in the island is so large to cause frequency instability (Kirschen *et al.*, 2003; Mousavi *et al.*, 2014); UFLS is conducted when the system frequency exceeds the acceptable threshold (Mousavi *et al.*, 2014);
- 6) performs load shedding when there is insufficient power generation capacity in the island;
- 7) quantifies the consequences of the cascading event. The following reliability measures for power system (Kirschen *et al.*, 2003; Billinton *et al.*, 2009) can be used as the indicators for the impact of cascading failure: DNS to the customers, total number of line tripping throughout the cascading process, number of customers affected.

Fig. 1 details the cascading failure analysis algorithm, which is described as the following steps:

- a) For each failure scenario:
 - initialize the system (topology, load/generation at each bus) with the output from the optimal power flow with the objective of generation costs minimization.
 - run random component failure (for each component, a random number is sampled, the component is failed, if the number is smaller than the failure probability of the component, p).
 - check for an island in the system based on the new topology.
- b) For each island:
 - perform a stability check, evaluate the system frequency deviation and the voltage magnitude of each bus.
 - apply UFLS if the frequency deviation exceeds the acceptable threshold (Mousavi *et al.*, 2014) (e.g., 2.5Hz).
 - restore load/generation balance through primary and secondary frequency control. Load shedding is implemented in case of generation capacity deficit.
 - run the DC power flow procedure.
 - remove lines with flow higher than the line tripping threshold α . If there are new islands, return to identification of islands and repeat the entire procedure, otherwise output the total power demand not served (DNS) to the customers and the number of lines

disconnected during the propagations of the cascading outage.

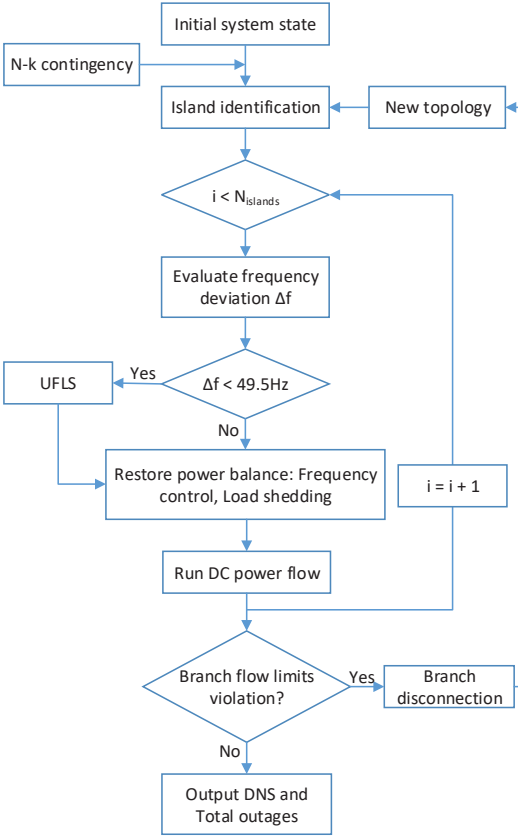


Fig. 1. Algorithm for cascading failure simulations

3. Calibration Approach for Model Validation

The cascading failure model uses multiple parameters such as random component failure probability p , and line tripping threshold α . These parameters can significantly affect the cascading outages propagation and its consequences. Therefore, it is critical that these parameters are calibrated to be the appropriate values when the analysis is applied to a specific system. Instead of calibrating the parameters in an intuitive way and checking the agreement between the simulation results and the historical data, an optimization procedure with the objective of minimizing the difference in statistics of the real and simulated cascades is applied.

In a previous study, we demonstrate that after calibration the component failure probability remained at the default value (0.001) during all test (Li *et al.*, 2018b). Therefore, in this study we focus

on the line tripping threshold α . Instead of a single parameter for every line, we grouped the WECC power system high-voltage lines into four groups (115 and 138 KV; 230 and 287 KV; 345 KV; 500 KV) and assigned a separate α for each of them. The possible range of each α is between 1 and 1.3 of the line tripping threshold.

The calibration is set such that aims at minimizing the difference between the distribution of DNS of the historical data and the distribution of DNS obtained by the simulations.

To estimate the difference between the two distributions we experiment with variety of methods, i.e. distance correlation (Szekely *et al.*, 2007), Kolmogorov-Smirnov test (Smirnov, 1948; Marsaglia *et al.*, 2003), Minkowski distance (Shahid *et al.*, 2009), and Kullback-Leibler divergence (Kullback and Leibler, 1951). The Minkowski distance and Kullback-Leibler divergence showed the most promising results. Therefore, they are elaborated in this paper.

The difference between the historical data and the simulation results using a generalized Minkowski distance is calculated as (Shahid *et al.*, 2009):

$$dif_E = \left(\sum \left| CCDF_{DNS_{DATA}}(dns_{DATA}) - CCDF_{DNS}(dns) \right|^p \right)^{1/p} \quad (1)$$

where $CCDF_{DNS_{DATA}}$ is complementary cumulative distribution function (CCDF) of the historical DNS, the $CCDF_{DNS}$ is the CCDF of the simulation results, and p is set to 1 in our computational experiments.

The difference between the historical data and the simulation results using the Kullback-Leibler divergence is calculated as (Kullback and Leibler, 1951):

$$\begin{aligned}
 dif_K &= \sum \left(CCDF_{DNS_{DATA}}(dns_data) \right. \\
 &\cdot \log \left(\frac{CCDF_{DNS_{DATA}}(dns_data)}{CCDF_{DNS}(dns)} \right) \Bigg) \\
 &+ \sum \left(CCDF_{DNS}(dns) \right. \\
 &\cdot \log \left(\frac{CCDF_{DNS}(dns)}{CCDF_{DNS_{DATA}}(dns_data)} \right) \Bigg). \quad (2)
 \end{aligned}$$

The cascading failure model calibration is defined as a single-objective optimization problem, which searches for the minimum of:

$$\min\{dif(\alpha_i)\} \tag{3}$$

where, *dif* is the calculated difference between the probability distributions of historical data and of simulation results (i.e. *dif_E* or *dif_K* in case either Eq. (1) or Eq. (2) is applied), and α_i are the line tripping thresholds for the four selected voltage levels.

Three optimization algorithms, GA, PSO-P and MADS, are selected to perform the simulation-based optimization required for the calibration of the cascading failure model. All of the optimization algorithms are chosen because of their capability to deal with simulation-based optimization problems (Fu, 2015).

Fig. 2 shows the flow chart of the calibration method.

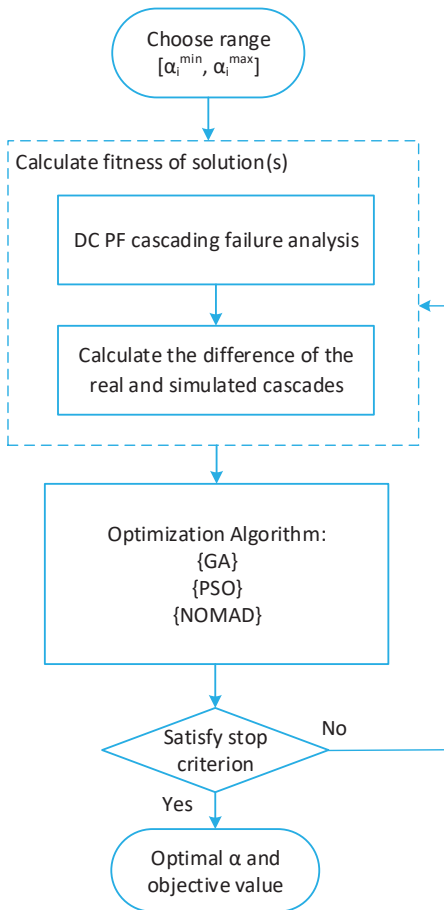


Fig. 2. Algorithm for the GA based calibration approach

The GA and PSO-P start with a population, with size N , of random values for α , determined using a uniform probability distribution:

$$pop = \begin{bmatrix} \alpha_{1,1} & \alpha_{1,2} & \alpha_{1,3} & \alpha_{1,4} \\ \alpha_{2,1} & \alpha_{2,2} & \alpha_{2,3} & \alpha_{2,4} \\ \vdots & \vdots & \vdots & \vdots \\ \alpha_{N,1} & \alpha_{N,2} & \alpha_{N,3} & \alpha_{N,4} \end{bmatrix} \tag{4}$$

where *pop* is the initial population and each row represents a potential solution for the optimization problem. Unlike GA and PSO-P, the nonlinear mesh adaptive direct search algorithm (NOMAD) starts with a single initial selection of the α parameters. The fitness value in Eq. (3), i.e. the difference between the distribution of DNS of the historical data and the distribution of DNS obtained by the simulations is calculated for each solution. The selected optimization algorithm processes the solutions and the fitness of the new solutions is assessed. The solutions with the best fitness continue in the next iteration. The procedure is stopped when the stopping criteria is reached. The functioning of each optimization algorithm is elaborated briefly in the following subsections.

3.1 Genetic algorithm

The GA is an evolutionary algorithm inspired by the natural genetics and the survival of the fittest. The GA is searching for better solutions by letting the fitter individuals to take over the population using a combination of stochastic process. The main GA operators are selection, crossover, mutation and replacement. In this study, we use tournament selection operator. As the name suggests, two or more randomly selected chromosomes (solutions) are entering a tournament. The solution with the highest fitness is selected to participate in the mating pool, i.e. the pool of solutions that will create the next population. The next population is created by applying blend crossover (BLX-0.5) operator and non-uniform mutation. The new and old population are compared and according to the fitness value and the best half of the population survives, the rest is deleted, i.e. elitist replacement. The GA used in this study is in-house made and elaborated in detail in (Gjorgiev and Čepin, 2013).

3.2 Particle swarm pattern search optimization

This algorithm combines particle swarm optimization (PSO) and the pattern search method. It begins with an initial population and uses one step of particle swarm at each search step. Successive iterations where the search steps work are reduced to successive iterations of particle swarm. However, if the search step is

unsuccessful, the poll step is applied to the best position over all particles, thus performing a local search in the poll set targeted at this point (Vaz and Vicente, 2007).

PSO is a swarm-based optimization algorithm developed by (Kennedy and Eberhart, 1995). The algorithm uses partial (solution) position and velocity in a search space as the main guiding criteria to the optimal solution. Each particle in the search space keeps track of its coordinates, which are linked with the fitness value of the best solution. This value is called *pbest*, and is stored for comparison. Furthermore, the optimizer tracks an additional "best" fitness value, obtained so far by the neighbors of any particle in the population. This location is called *lbest*. When a particle takes all the population as its topological neighbors, the best value is a global best and is called *gbest*. At each iteration, the algorithm changes the velocity (acceleration) of each particle towards *pbest* and *lbest*.

For the purpose of this study, we use the Particle Swarm Pattern Search (Vaz and Vicente, 2007) method integrated in the OPTI toolbox (Currie, 2018).

3.3 Mesh adaptive direct search algorithm

MADS is an algorithm for solving non-linear and non-convex optimization problems. The algorithm iterates on a series of meshes with varying size. The mesh represents a discretization of the space of variables. Furthermore, the algorithm performs an adaptive search on the meshes as well as controlling the refinement of the meshes. The MADS algorithm is an extension of the Generalized Pattern Search (GPS) class, by permitting local exploration, which is known as polling (Audet and Dennis, 2006). The polling is performed in a set of directions in the optimization variables space. For the purpose of this paper, we use the NOMAD software (Digabel, 2011; Audet *et al.*, 2009) that implements the MADS for blackbox optimization. NOMAD is also used as a part of the OPTI toolbox.

4. Analyses and results

For validation and calibration of the cascading failure model we use the reduced 240-bus WECC network system (Price and Goodin, 2011). The system includes the hourly profiles for load demand and RES power generation for 2004. The existing 17 coal-fired and 4 nuclear power plants are treated as base load units. The hourly

generation dispatch of 50-aggregated gas fired power plants are obtained by an optimal power flow using generator capacity limits and cost information.

In the WECC network, the main source of blackouts data is the frequency of different blackouts size from 1984 to 2006 (NERC, 2004), which is provided by the North American Electrical Reliability Council (NERC).

The hourly load consumption at each bus of the WECC network is provided. Representative hours from the peak load and off-peak load condition are sampled for performing the cascading failure simulations. For each hour, 1000 initial contingencies of random line and transformer failures are simulated to trigger cascading events.

The cascading failure model and the calibration method are coded in the MATLAB-R2015b environment. The analyses are performed on Intel(R) Core(TM) i9 CPU.

Initially, we run the cascading failure model on the WECC system for validation purpose. The default line tripping threshold of $\alpha_i = [1 \ 1 \ 1 \ 1]$ is set for all four groups of lines. The obtained results for the cumulative distributions of the DNS are given in Fig. 3.

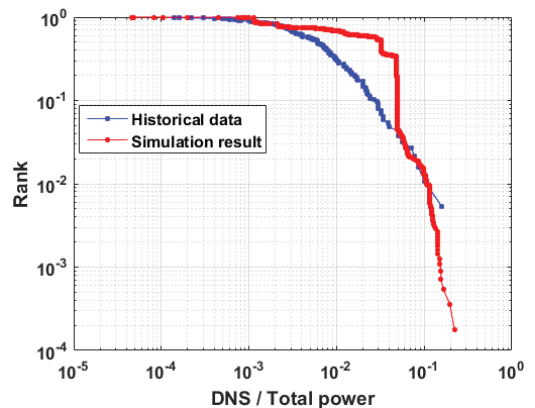


Fig. 3. Cumulative distribution of the DNS obtained with the cascading failure model for default α .

The difference of the distributions according to the Minkowski distance is 1.376, and according to Kullback-Leibler divergence is 1.228. Note that these values are obtained by different objective functions (Eq. (1) and Eq. (2)), therefore, one should not directly compare them.

Fig. 4 a) and b) show the results obtained by the GA with the Minkowski and Kullback-Leibler divergence based objective functions, respectively. Fig. 4 a) and b) show a significant improvement of the simulation results compared to the default scenario (Fig. 3) when the line failure

rates are equal to one. When the Minkowski distance (Eq. (1)) is used as an objective function (see Fig. 4 a)), the obtained line tripping thresholds are $\alpha = [1.154, 1.2689, 1.1308, 1.1631]$, and objective function values, $dif_E = 0.0135$ and $dif_K = 0.0319$. When the Kullback-Leibler divergence (Eq. (2)) is used as an objective function (see Fig. 4 b)), the obtained line tripping thresholds are $\alpha = [1.1538, 1.2693, 1.2954, 1.1522]$, and objective function values, $dif_E = 0.0347$ and $dif_K = 0.0167$. The results does not clearly show which of the objective function provide better calibration. However, it is clear that the model calibration using any of the objective functions can provide good statistical match between the historical data and the simulation results. The average runtime of the GA is 22 hours.

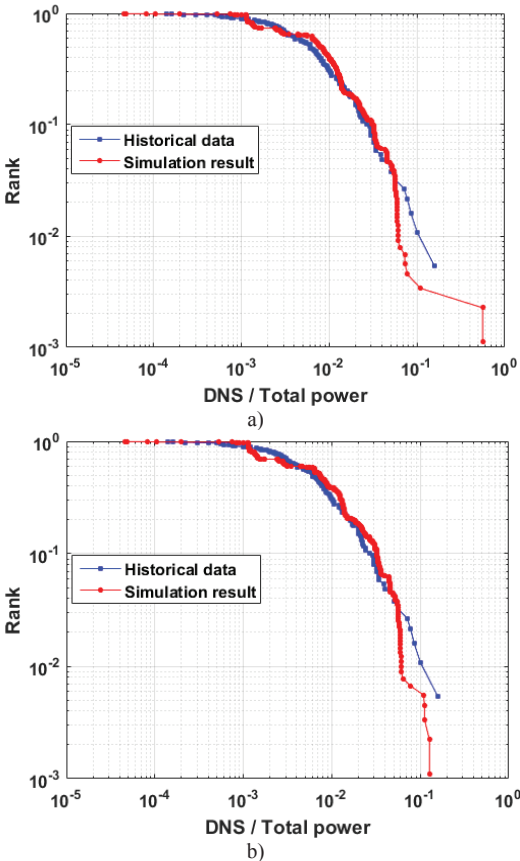


Fig. 4. Cumulative distribution of the DNS obtained with GA with: a) Minkowski distance; b) Kullback-Leibler divergence objective functions.

Fig. 5 a) and b) shows the results obtained by the PSO-P with the Minkowski and Kullback-Leibler divergence based objective functions, respectively. When PSO-P is used as an optimizer

and the Minkowski distance (Eq. (1)) as an objective function (see Fig. 5 a)) the line tripping thresholds are $\alpha = [1.2540, 1.2844, 1.3000, 1.0134]$, and objective function values, $dif_E = 0.0441$ and $dif_K = 0.03981$. When the Kullback-Leibler divergence (Eq. (2)) is used as an objective function (see Fig. 5 b)), the obtained line tripping thresholds are $\alpha = [1.1968, 1.2932, 1.1369, 1.1630]$, and objective function values, $dif_E = 0.1721$ and $dif_K = 0.0673$. In this case, it is clear that the solution obtained with Minkowski distance as an objective function is the better one. Furthermore, even though a significant improvement is achieved compared to the default scenario (Fig. 3), it is clear that the GA obtained better results than the PSO-P. With an average runtime of 57 hours, the PSO-P is a significantly slower compared to the GA.

Fig. 6 a) and b) shows the results obtained by the NOMAD with the Minkowski and Kullback-Leibler divergence based objective functions, respectively.

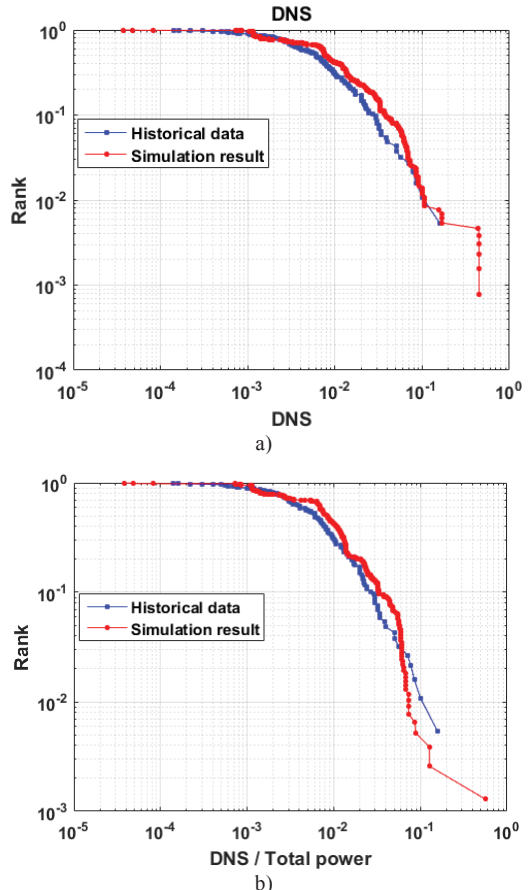


Fig. 5. Cumulative distribution of the DNS obtained with PSO-P with: a) Minkowski distance; b) Kullback-Leibler divergence objective functions.

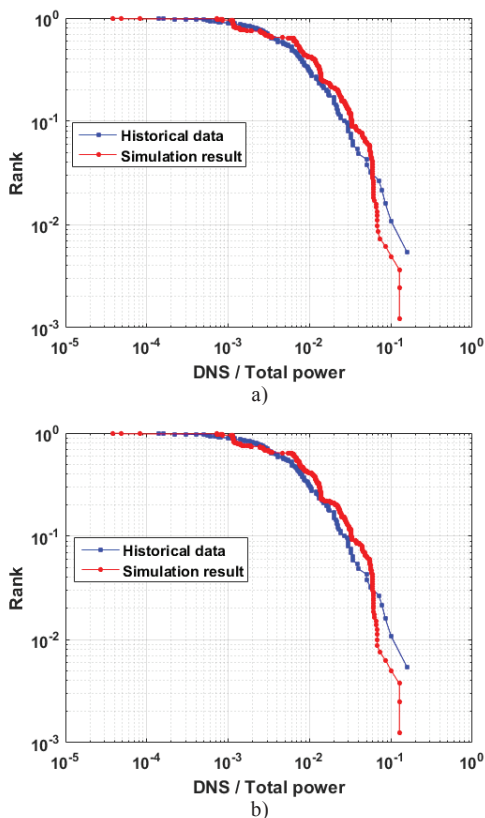


Fig. 6. Cumulative distribution of the DNS obtained with NOMAD with: a) Minkowski distance; b) Kullback-Leibler divergence objective functions.

When NOMAD is used as an optimizer and the Minkowski distance (Eq. (1)) as an objective function (see Fig. 6 a)) the line tripping thresholds are $\alpha = [1.2860, 1.2795, 1.3, 1.1440]$, and objective function values, $dif_E = 0.1641$ and $dif_K = 0.0468$. When the Kullback-Leibler divergence (Eq. (2)) is used as an objective function (see Fig. 6 b)), the obtained line tripping thresholds are $\alpha = [1.2772, 1.2791, 1.3, 1.1520]$, and objective function values, $dif_E = 0.1484$ and $dif_K = 0.0398$. In this case, it is clear that the solution obtained with Kullback-Leibler divergence as an objective function is the better one. Even though a significant improvement is achieved compared to the default scenario (Fig. 3), it is clear that the GA obtained better results than the NOMAD algorithm. Furthermore, we performed multiple trials with the NOMAD, practically tested all poll-direction types and used smaller poll and mesh sizes than the defaults. However, NOMAD did not get as good solutions as the GA. With an average runtime of 32 hours,

the NOMAD is slower compared to the GA and faster compared to the PSO-P.

5. Conclusions

In an attempt to validated and calibrate a cascading failure simulation model, we experimented with different optimization algorithms and objective functions. We used GA, PSO-P and NOMAD as optimizers and Minkowski distance and Kullback-Leibler divergence objective functions. The results show advantage of the GA over PSO-P and NOMAD. However, both Minkowski distance and Kullback-Leibler divergence objective functions performed similarly with no conclusive advantage of one over the other.

References

Audet, C. & Dennis, J. E. (2006). Mesh Adaptive Direct Search Algorithms for Constrained Optimization. *SIAM J. on Optimization* 17(1): 188-217.

Audet, C., Digabel, S. L. & Tribes, C. (2009). NOMAD user guide. Technical Report G-2009-37, Les cahiers du GERAD.

Billinton, R., Gao, Y. & Karki, R. (2009). Composite system adequacy assessment incorporating large-scale wind energy conversion systems considering wind speed correlation. *Power Systems, IEEE Transactions on* 24(3): 1375-1382.

Bing, L., Sansavini, G., Bolognani, S. & Dörfler, F. (2016). Linear implicit AC PF cascading failure analysis with power system operations and automation. In *2016 IEEE Power and Energy Society General Meeting (PESGM)*, 1-5.

Carreras, B. A., Newman, D. E., Dobson, I. & Degala, N. S. (2013). Validating OPA with WECC Data. In *HICSS*, 2197-2204.

Currie, J. (2018). OPTI Toolbox: <https://inverseproblem.co.nz/OPTI/index.php/DL/License>.

Digabel, S. L. (2011). Algorithm 909: NOMAD: Nonlinear Optimization with the MADS Algorithm. *ACM Trans. Math. Softw.* 37(4): 1-15.

Ferc, N. (2012). Arizona-southern california outages on 8 September 2011: causes and recommendations. *FERC and NERC*.

Fu, M. C. (2015). *Handbook of Simulation Optimization* New York, NY: Springer.

- Gjorgiev, B. & Čepin, M. (2013). A multi-objective optimization based solution for the combined economic-environmental power dispatch problem. *Engineering Applications of Artificial Intelligence* 26(1): 417-429.
- Goldberg, D. (1989). *Genetic Algorithms in Search, Optimization and Machine Learning*. Reading, MA: Addison-Wesley Professional.
- Kennedy, J. & Eberhart, R. (1995). Particle swarm optimization. In *Proceedings of ICNN'95 - International Conference on Neural Networks*, Vol. 4, 1942-1948 vol.1944.
- Kirschen, D., Bell, K., Nedic, D., Jayaweera, D. & Allan, R. (2003). Computing the value of security. In *Generation, Transmission and Distribution, IEE Proceedings-*, Vol. 150, 673-678: IET.
- Kullback, S. & Leibler, R. A. (1951). On Information and Sufficiency. *Ann. Math. Statist.* 22(1): 79-86.
- Kundur, P., Balu, N. J. & Lauby, M. G. (1994). *Power system stability and control*. McGraw-hill New York.
- Li, B., Barker, K. & Sansavini, G. (2018a). Measuring Community and Multi-Industry Impacts of Cascading Failures in Power Systems. *IEEE Systems Journal* 12(4): 3585-3596.
- Li, B., Gjorgiev, B. & Sansavini, G. (2018b). Meta-Heuristic Approach for Validation and Calibration of Cascading Failure Analysis. In *2018 IEEE International Conference on Probabilistic Methods Applied to Power Systems (PMAPS)*, 1-6.
- Li, C., Sun, Y. & Chen, X. (2007). Analysis of the blackout in Europe on November 4, 2006. In *Power Engineering Conference, 2007. IPEC 2007. International*, 939-944: IEEE.
- Marsaglia, G., Tsang, W. W. & Wang, J. (2003). Evaluating Kolmogorov's Distribution. *Journal of Statistical Software* 008(i18).
- Mousavi, O. A., Bozorg, M., Cherkaoui, R. & Paolone, M. (2014). Inter-area frequency control reserve assessment regarding dynamics of cascading outages and blackouts. *Electric Power Systems Research* 107: 144-152.
- NERC (2004). Information on Blackouts in North America, Disturbance Analysis Working Group (DAWG) Database: <http://www.nerc.com/~dawg/database.html>.
- North American Electric Reliability Council (NERC).
- Price, J. E. & Goodin, J. (2011). Reduced network modeling of WECC as a market design prototype. In *2011 IEEE Power and Energy Society General Meeting*, 1-6: IEEE.
- Romero, J. J. (2012). Blackouts illuminate India's power problems. *IEEE spectrum* 49(10).
- Sansavini, G., Piccinelli, R., Golea, L. & Zio, E. (2014). A stochastic framework for uncertainty analysis in electric power transmission systems with wind generation. *Renewable Energy* 64: 71-81.
- Shahid, R., Bertazzon, S., Knudtson, M. L. & Ghali, W. A. (2009). Comparison of distance measures in spatial analytical modeling for health service planning. *BMC health services research* 9: 200-200.
- Smirnov, N. (1948). Table for Estimating the Goodness of Fit of Empirical Distributions. *Ann. Math. Statist.* 19(2): 279-281.
- Staszewski, L. & Rebizant, W. (2010). The differences between IEEE and CIGRE heat balance concepts for line ampacity considerations. In *Modern Electric Power Systems (MEPS), 2010 Proceedings of the International Symposium*, 1-4: IEEE.
- Szekely, G. J., Rizzo, M. L. & Bakirov, N. K. (2007). Measuring and testing dependence by correlation of distances. *Ann. Statist.* 35(6): 2769-2794.
- Vaiman, M., Bell, K., Chen, Y., Chowdhury, B., Dobson, I., Hines, P., Papic, M., Miller, S. & Zhang, P. (2012). Risk assessment of cascading outages: Methodologies and challenges. *Power Systems, IEEE Transactions on* 27(2): 631-641.
- Vaz, A. I. F. & Vicente, L. N. (2007). A particle swarm pattern search method for bound constrained global optimization. *J Glob Optim* 39(197).